Developing an Apparatus to Study the Kinetics of Sulfide Oxidation

Noah Bowman

27 November, 2013

GEOL 394

Advisors: Dr. J. Farquhar and D. Eldridge

Table of Contents

Abstract

Oxidation of H_2S is complex and involves the formation of numerous sulfur compounds with intermediate oxidation states, including thiosulfate, sulfite, polysulfides, and elemental sulfur.

This thesis describes work to develop an experimental apparatus and procedure for running sulfide oxidation experiments. We inject a small aliquot (~5ml) stock (0.2M) solution of Na_2S previously prepared under a pure nitrogen atmosphere into a reaction chamber consisting of a buffer solution of 5 mM Na_2CO_3 and $NaHCO_3$ and a stir bar, previously bubbled with oxygen for 30 minutes. This reaction chamber is immersed in a water bath kept at a constant 25°C using a VWR temperature bath. The reaction chamber is pressurized to 0.1 kg/cm^3 above atmospheric pressure using an oxygen tank connected to two regulators, one for small scale adjustments, and another for large scale adjustments. Sampling occurs every 3 hours over a period of 60 hours, with three breaks of about 6-8 hours. Sampling is carried out in triplicate. Points are averaged and the standard deviation is used as the error of each point. We use the technique outlined in Cline (1969) to make our measurements of sulfide concentration.

The intended use of the apparatus being designed is to constrain the kinetics of sulfur oxidation. Additionally, it will be used in future projects that will look at isotope effects of the reaction. An important aim of this thesis is to design an experimental apparatus that is capable of giving accurate and consistent data for oxidation of sulfide and other sulfur species. Uncertainties arising in experiments from sampling procedures and concentration measurements were evaluated and suggest that difficulties in experimental design arise as a result of aberrations caused by oxygen partial pressure variation and trace metal contamination.

1. Introduction

Misc. Background

Sulfide is a common waste product of the metabolisms of anaerobic bacteria, which use sulfate ions as the electron acceptor. Hydrogen sulfide is found to be produced in a variety of places, including the pore waters of sediments and stagnant basins, such as rivers, fjords, lakes, and seas; and in deep sea hydrothermal vents (Zopfi, 2004).

Most of the sulfide produced in marine sediments is eventually oxidized back to sulfate through a series of sulfur compounds of intermediate oxidation state. This series of reactions that produce the sulfur compounds of intermediate oxidation state can vary as the pathway from sulfide to sulfate is a complex web of competing reactions (Zopfi, 2004). Interest in understanding the role of sulfide oxidation in natural environments arises because of its importance as a pathway for converting sulfur in marine sediments and also because of the complexity of its chemistry. One of the fundamental parameters that determines importance is the rate at which sulfide oxidation occurs in natural environments (Chen and Morris, 1972). Another aspect of sulfide oxidation that may be important relates to tracing changes these rates that arise because of other environmental factors. This study seeks to develop an experimental apparatus that can be used to study sulfide oxidation, and the isotopic signatures of sulfide oxidation under different environmental conditions, specifically the ^{33}S and ^{36}S isotopes. The broader impacts of this work are therefore related to developing an apparatus that can be used to understand an important process that occurs in the oceans.

Marine sulfur geochemistry

In the marine environment, sulfur predominantly exists as dissolved sulfate (oxidation state VI), and sulfide and pyrite (oxidation states I and II, respectively). The reduction of sulfate to sulfide in marine sediments, and sometimes the water column, initiates the processes that lead to pyrite formation. This process also generates a characteristic isotopic fractionation for sulfur isotopes that accounts for the depletion of ^{34}S of marine pyrite when compared to oceanic sulfate. A significant proportion (70-90%) of this sulfide is reoxidized back to sulfate. The reoxidation process generates sulfur compounds of intermediate oxidation state. A large variety of sulfur compounds of intermediate oxidation state exist between these two end members (at trace amounts). Though these intermediates hold little influence in terms of concentration, they are broadly influential in terms of trace metal solubility (through complexation with polysulfides and thiosulfate) (Jacobs and Emerson, 1982; Morse et al., 1987). These intermediates are rapidly cycled and it has been shown that the bacterial disproportionation reactions of sulfite, thiosulfate, and elemental sulfur have a significant effect on the fractionation of stable sulfur isotopes, further amplifying the ^{34}S depletion of Marine Pyrite (Jørgensen, 1990; Canfield and Teske, 1996).

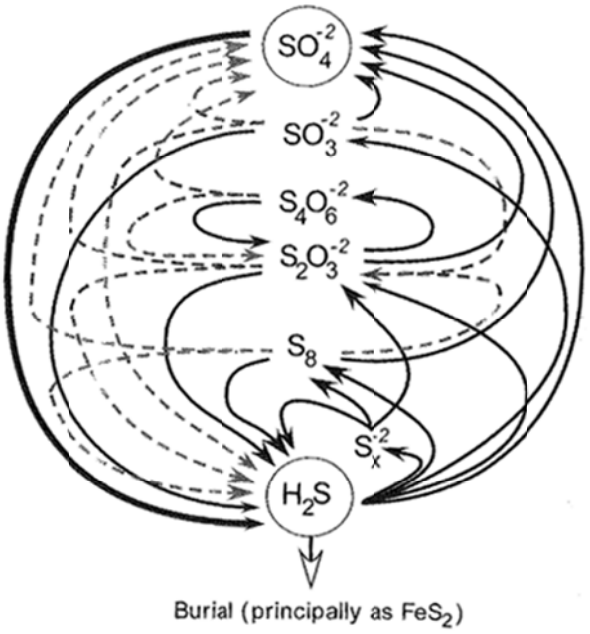

Figure 1: Schematic of sedimentary sulfur cycle. Left side downward pointing arrow are reductive processes, Right side

upward pointing arrows are oxidative processes, dashed lines are bacterial disproportionation reactions. From Zopfi (2004).

Sulfur intermediates in the marine realm are primarily produced by the oxidation of sulfide during bacterial sulfate reduction. 10-20% of the produced sulfide is buried, (principally as pyrite sulfur) and the remaining 80-90% is recycled back into the complex web of chemical and biological sulfur reactions (Jørgensen, 1987; Fossing and Jørgensen, 1987; Jørgensen and Bak, 1991).

Oxic sulfide oxidation

When dissolved sulfide comes into contact with oxygen, sulfide may be oxidized according to the overall reaction:

$$HS^- + 2O_2 \rightarrow SO_4^{2-} + H^+ \qquad (1)$$

This reaction is however more complex than this simple reaction and involves several intermediate steps. While the exact nature of these reactions are unknown (Zhang and Millero, 1993), a significant amount of information exists about them. Sulfite is an important product produced by:

$$HS^- + 1.5O_2 \rightarrow HSO_3^- \qquad (2)$$

Sulfite rapidly oxidizes to form sulfate: SO_3^{2-}+ $0.5O_2$→ SO_4^{2-}. Thiosulfate can also be formed by the reaction of sulfite and HS^-: HS^-+ SO_3^{2-} + $0.5O_2$ → $S_2O_3^{2-}$+ OH^-. In many experiments, sulfate and thiosulfate are the only stable oxidation products that accumulate.

It has been proposed that tetrathionate, $S_4O_6^{2}$, is an intermediate to the oxidation of sulfite to thiosulfate. Tetrathionate would be produced in the presence of oxidants like O_2, Fe(III), Mn(IV), and I_2. Pyrite can catalyze the reaction of O_2 and $S_2O_3^{2-}$ (Xu and Schoonen, 1995) at pH less than 8.6.

With trace metals present, elemental sulfur can be formed in the initial steps of sulfide oxidation by:

$$2HS^- + O_2 \rightarrow 2S^0 + 2OH^- \qquad (3)$$

(Steudel, 1996; Zhang and Millero, 1993)

This elemental sulfur can react with sulfite and sulfide to form thiosulfate and polysulfides by the following reactions:

$$S^0 + SO_3^{2-} \rightarrow S_2O_3^{2-} \qquad (4)$$

and

$$(n-1)S^0 + HS^- \rightarrow HS_n^- \qquad (5)$$

respectively.

According to Steudel et al., 1986, polysulfides are unstable in the presence of oxygen and decompose to elemental sulfur and thiosulfate. The reactions that transform sulfide and sulfate are generally initiated by a reaction like reactions (1) and (2) and depend on the availability of oxygen. The rates also have a strong dependence on the concentration of sulfide. Zhang and Millero (1991), Zhang et al., (1993), and Luther et al., (2011) also demonstrated the rates have a strong dependence on the concentration of trace metals

The oxidation of sulfide in seawater is overall 1st order with respect to sulfide and oxygen, meaning that the oxidation is directly proportional to the concentration of sulfide and dissolved oxygen. Major products of this reaction are SO_4^{2-}, SO_3^{2-}, and $S_2O_3^{2-}$, their relative distributions dependent on pH (Zhang and Millero, 1993).

The pH of the media is also important in determining portions of sulfur compounds produced by sulfide oxidation and has a possible influence on the rates. A 1972 study by Chen and Morris studied the oxidation of H_2S in pure water. They found that the reaction rate relation to pH is

complicated, with two maxima. They postulated that the complicated pH dependence is due to a free-radical chain reaction with sulfur as the end product. This sulfur combines with S^{2-} to make unstable polysulfides. Evidence for polysulfide formation was found through UV absorption measurements, however only at pHs lower than 7.2.

O'Brien and Birkner in 1977 studied sulfide oxidation in pure water at pH= 7.55. They found that a low initial ratio of sulfide to oxygen favors sulfate, thiosulfate, and sulfite production. Conversely, they found a high initial ratio of sulfide to oxygen favors the production of elemental sulfur and polysulfides (with total sulfide concentration greater than 1 mM).

Polysulfide can qualitatively be detected by the appearance of a yellow-green color. Quantitative detection is complicated due to the high reactivity of polysulfide compounds.

The overall rate equation for the oxidation of hydrogen sulfide can be represented:

$$-\frac{d[H_2S]}{dt} = k[H_2S]^a[O_2]^b \quad (6)$$

where k is the overall rate constant and a and b are the order of reaction and the brackets represent concentrations. If oxygen is present in excess, the rate equation can be further reduced to a pseudo rate equation:

$$-\frac{d[H_2S]}{dt} = k'[H_2S]^a \quad (7)$$

k' can be related to k by

$$k' = k[O_2]^b \quad (8)$$

The pseudo rate law can be used to calculate the true rate constant by collating experiments run at different partial pressures of O_2 (in excess). The k' value of successive experiments that differ only in their oxygen partial pressure are plotted in log(SII) vs. time space and the intercept of the line of best fit through them is the k value for the true rate law k. It is more precise to measure k this way, through k'. More variables are controlled during the course of the experiment.

Zhang in 1991 tested the reaction at a pH of 8.2, 0.002 M of bicarbonate, and 45°C. Elemental sulfur and polysulfides were not found. Sulfite, thiosulfate, and sulfate were produced. The initial product was sulfite, with a proportion decreasing as the reaction wore on. After running the reaction for 60 hours, thiosulfate was the most abundant product. This indicates that the reaction does not go to completion in alkaline waters. Thiosulfate is known to be stable in neutral and alkaline waters containing oxygen.

At a pH of 4, the major product of the reaction is sulfate. The maximum rate of oxidation of sulfite occurs at a pH of 6.5 (Zhang and Millero, 1993).

Sulfide oxidation in nature

The modern Black Sea is an example of an anoxic and euxinic (sulfidic) environment. According to Canfield and Raiswell (1999), the Earth's oceans have been anoxic/suboxic and euxinic for long periods of time in the past. Studying modern euxinic and anoxic/suboxic euxinic environments can provide insight into the ancient pre-oxygenated oceans and early eukaryote evolution when sulfur metabolisms were first developing.

Sulfide oxidation can be mediated biologically or abiologically by various eukaryotes and various metal compounds such as Fe(III, II) and Mn(III, IV) respectively. In abiologic and biologic sulfur oxidation, trace metals help overcome the kinetic barrier. Trace metals such as Fe(II) and Mn(II) are oxidized to Fe(III) and Mn(III, IV), which act as electron receptors for sulfur, regenerating Fe(II) and Mn(II) in the process (Luther et al., 2011).

In addition to marine environments like lakes, fjords, seas, deep sea hydrothermal vents, and pore waters of sediments and stagnant basins, sulfide is also produced in nonmarine environments, including volcanoes, thermal pools and springs associated with volcanic activity. Yellowstone National Park, in Wyoming, is a large caldera that has a number of hydrothermal springs, pools, geysers, and other sulfidic hydrothermal systems. Sulfide in the systems is generated by a combination of volcanic sources and in some places metabolic activity (Schoen and Rye, 1970). The presence of sulfide in springs and pools that exists beneath the surface provides an environment for sulfide oxidation. Interest in understanding the isotopic fractionations associated with sulfide oxidation under conditions similar to those seen at Yellowstone is provided by ongoing studies of Alexey Kamyshny and the Farquhar lab. A question that exists is whether it is possible to constrain the role of biological processes in sulfide oxidation.

In Yellowstone, Hydrogen Sulfide is abiologically oxidized to sulfur and sulfur is biologically oxidized to sulfuric acid. However, at Mammoth Hot Springs, hydrogen sulfide is biologically oxidized to sulfur. Previous studies suggested that bacteria might produce all of the sulfuric acid (Schoen and Rye, 1970).

Sulfur isotope fractionation during sulfide oxidation

Masses of the S^{32} and S^{34} nuclei are different and these isotopes react at different rates in chemical reactions such as those associated with sulfide oxidation. If, during the formation of sulfur compounds, the reaction does not consume the reactants in their entirety, the products will have a different ratio of isotopes than the remaining reactants. In this enrichment or depletion of one of the isotopes, information about the genesis of the sulfur compounds can be inferred.

Oxidation reduction reactions where organisms participate also show deviations in the proportion of isotopes of the reactants and products.

Laboratory experiments on sulfur isotope fractionation by sulfur oxidizing bacteria show $\delta^{34}S$ fractionations of about -6 per mil in sulfur formed from hydrogen sulfide and -6 to -18 per mil in sulfate formed from hydrogen sulfide.

Laboratory experiments on the biological oxidation of sulfur to sulfate show $\delta^{34}S$ fractionations of 0 to +2 per mil. In contrast, equilibrium inorganic oxidation of hydrogen sulfide to sulfate show large positive fractionations (68.0 per mil at 25°C and 48.0 per mil at 100°C) (Sakai, 1957).

Some studies in geothermal areas show that inorganic oxidation of hydrogen sulfide to sulfur does not appreciably change the proportion of sulfur isotopes (Fry et al., 1988), but relatively few experimental studies have been done. There are even fewer studies calibrating isotope effects associated with the rarest isotopes (^{33}S and ^{36}S). The apparatus being designed will ultimately be used to calibrate these fractionations.

The isotopic variation in hydrothermal settings where sulfide oxidation occurs is measurable, but not large. Mammoth Hot springs is unusual in Yellowstone in that the surrounding rocks are sedimentary rather than volcanic. The hot springs deposits are travertine rather than siliceous sinter. Mammoth has temperatures below 70°C, in contrast with temperatures of over 90°C at the other springs. Also, the emission of hydrogen sulfide is much slower at Mammoth than the other springs. As such, these conditions may favor biogenic oxidation of hydrogen sulfide by bacteria. Isotopic measurements may help to resolve this issue (Schoen and Rye, 1970).

In 1957, Sakai measured the $^{34}S/^{32}S$ ratio in about 90 samples. He found that the sulfates formed two clear groups, heavy and light. The heavy sulfate was from igneous and seawater sources and the light sulfate was secondary, formed from the oxidation of sulfides on the earth's surface.

Low temperature oxidation

In other settings, it may also be possible to determine whether sulfide oxidation is biological or a biological using sulfur isotope fractionations. Work by Zerkle et al. (2010) and Canfield et al., (2010) show two different types of isotope profiles of sulfide in different lakes: Green Lake near Fayettville, NY and Lago di Cadagno in the Piora Valley in Switzerland. The profile of Green Lake (Zerkle et al. (2010) shifts to ^{34}S enriched compositions in regions where sulfide oxidation occurs; whereas in Lago di Cadagno, (Canfield et al., 2010) the profile for sulfide shifts to ^{34}S depleted compositions in regions where sulfide oxidation occurs. This difference has been interpreted to reflect differences in the relative proportion of biological to abiological oxidation pathways. The apparatus designed here will be used to calibrate the abiological reactions for all four sulfur isotopes, and ultimately to provide information that can be used to test this hypothesis. Similar profiles have been measured in Marine settings (e.g., Li et al., 2010) and provide another use for this information.

Hypothesis

It is the goal of these experiments to construct an apparatus that is able to oxidize sulfur in a closed environment at a constant temperature. We use the experiments by the Millero group in 1993 as the basis for our design. However, the end goal of our experiments is to measure isotopic fractionation of sulfur. This requires that we use a higher starting concentration of dissolved sulfur, so we have enough material to measure in the mass spectrometer. The hypotheses at the start of this study were:

1. The increased starting sulfide concentration will not affect the kinetics of the reaction, as described by Zhang and Millero (1991). First order kinematics will be observed, with a rate constant consistent with their experiments.
2. Our reaction vessel will function properly, keeping oxygen at a constant concentration and keeping temperature of reaction vessel constant.

A number of complications were encountered over the course of this work to design the apparatus, which led to many revisions of the working hypotheses. Some of the experiments yielded rates that were inconsistent with a simple control by either oxygen or sulfide. Two further working hypotheses were developed as a result of these complications. First, the rate laws determined by the individual experiments were very difficult to fit, and a hypothesis was developed that can be stated as:

3. The experimental noise reflects poor control on the oxygen partial pressure in the system, and therefore causes changes in the rates between sampling points.

This hypothesis was tested by conducting experiments with improvements in pressure regulation, with the addition better valves to prevent leakage of oxygen. Once the oxygen control was refined, the rate laws determined in different experiments did not follow a simple relationship with respect to oxygen partial pressure. This led to the hypothesis that:

4. Catalysis by trace metals or some other contaminants was influencing the experiments.

This second hypothesis has not yet been tested, but tests are proposed at the end of this thesis.

2. Methods

Cline chemistry for quantifying hydrogen sulfide concentrations

The Methylene Blue method of detecting and quantifying hydrogen sulfide has been widely used since it was first devised by Fischer in 1883. As described by Fischer, the Methylene Blue method is somewhat erratic. In 1968, Strickland

and Parsons introduced a refinement of the Methylene Blue method that is easily standardized, applicable to a wide range of concentrations, and free of salt effects and temperature dependence.

Table 1. Suggested reagent concentrations and dilution factors, (recipes for Cline solution), to use to determine sulfide sulfur. From Cline (1969).

Sulfide Concentration(µmoles/liter)	Diamine concentration(g/500ml)	Ferric concentration (g/500ml)	Dilution Factor (ml:ml)	Path Length (cm)
1-3	0.5	0.75	1:1	10
3-40	2.0	3.0	1:1	1
40-250	8.0	12.0	2:25	1
250-1000	20.0	30.0	1:50	1

The reagents used are N, N-dimethyl-p-phenylenediamine sulfate and ferric chloride ($FeCl_3 \cdot 6H_2O$).

To prepare the Cline solution, the two reagents are dissolved in 500 ml of cool 50% reagent grade hydrochloric acid. The solution is stable for several months, particularly if stored in a dark bottle under refrigeration. The 2nd recipe on the table was used for these experiments.

Applications of the Cline Method to Sampling

When sampling the reaction vessel, it is important to minimize nitrogen exposure which would change the partial pressure of oxygen in the experiment. A sample syringe is flushed six times with pure oxygen, and then the solution is carefully extracted from the reaction vessel, carefully to not agitate the solution (minimizing mixing with headspace oxygen). The solution is then pipetted into a solution of zinc acetate, which fixes the hydrogen sulfide as zinc sulfide, after which the sulfide will no longer oxidize nor degas from solution. An aliquot of the prepared Cline solution is then added to the fixed zinc solution to form Methylene Blue, which is quickly capped and mixed to minimize volatilization of the hydrogen sulfide during the reaction. After 30 minutes, the absorbance of the Methylene blue solution is measured spectrophotometrically in a Spectro UV-UIS Dual Beam 8 Auto Cell UVS 2800 from Labomed, Inc.

Absorbances are then related to concentration using a calibration curve. The calibration curve is calculated through careful preparation of a sulfide solution. Several dilutions at different concentrations ranging from 5 mM to 40 mM are made from this solution. Each dilution is then injected with the appropriate amount of Cline solution and spectrophotometrically measured for absorbance. These samples with different absorbances are graphed on a plot of absorbance vs. concentration. The slope of the line of best fit through these points is used as the conversion factor.

Experimental Protocol

Approximately 5 ml of 0.1 M Na_2S solution is injected into a reaction vessel filled with a 1 liter, 5 mM solution of Na_2CO_3 and $NaHCO_3$ that had been bubbled with oxygen for 30 minutes. The reaction vessel, a closed container, is immersed in a water bath kept at a constant 25° C. The water bath is rated to a precision of ± 0.01° C by its manufacturer. The reaction solution is mixed throughout the duration of the experiments with a magnetic stir bar. The reaction vessel is plumbed with two entry points on the stopper. One is connected to an oxygen tank and pressure regulator that keeps headspace pressure in the reaction vessel at a constant 0.1 kg/cm^2 above

atmospheric pressure. The other is used to sample the solution.

3. Results

A summary of the timeline of the experiments is included in the appendix (as a table).

The first experiment was SII-O2-exp1. The reaction was buffered by a 0.1M solution of $Na_2HPO_4 \cdot 12H_2O$. The solution was bubbled with pure oxygen for 30 minutes. 25 ml of a stock solution of 0.2M Na_2S (5 mM) was injected into the reaction vessel to begin the experiment. We set the pressure regulator to 3 psi, it rose to 5 psi, and we kept it at 5 psi. The pressure regulator wouldn't keep it precisely at 5 psi reliably, so it had to be manually adjusted from time to time.

The data was most consistent with 2nd order kinetics with respect to sulfide (2nd order, k_{pseudo}=0.5131, R^2 = 0.9877). These results go against results obtained by Zhang and Millero in 1993, who found that the relationship is 1st order with respect to sulfide. They used a different buffer, carbonate, (seawater concentration, ~2.3 mM (Zeebe, 2011)), and a different starting amount of sulfide (25 µM).

The second experiment, SII-O2-exp2 followed the design of the first solution, but instead of a 0.1M buffer of $Na_2HPO_4 \cdot 12H_2O$, a 0.2M buffer was used. The reaction was monitored at a more regular rate, sampling every three hours through the night instead of every hour during the day. The reaction proceeded at a slower rate than the previous experiment (2nd order, k_{pseudo}=0.366, R^2=0.9828). We think that the higher concentration of buffer is responsible for the slowed rate.

The third experiment, SII-O2-exp2α, was a repeat of the second experiment, to test if the experimental design would give reproducible results. The results were comparable (2nd order, k' = 0.3113, R^2 = 0.9924). However, at this time it became apparent that phosphate buffers aren't the best for the pH range encountered in this experiment. Additionally, phosphate buffered waters aren't normally encountered in nature. The better buffer would be an equal parts carbonate and bicarbonate buffer. This buffer is optimum for the pH range of these experiments and is ubiquitous in nature. We had initially avoided this buffer due to concerns that small amounts of the buffer would degas (as CO_2) during the course of the experiment.

The fourth experiment, SII-O2-Carb-exp1, followed the design of the previous experiment but instead used an equal parts carbonate-bicarbonate buffer (50 mM each). The results were ambiguous (2nd order k' = 0.1157, R^2 = 0.9183).

The fifth experiment, SII-O2-200-exp1, brought the following modifications; overhead pressure reduced to 1.5 psi above atmospheric pressure, carbonate-bicarbonate buffer reduced to 5 mM, and starting amount of sulfide reduced to ~200 mM. This experiment showed more consistent results than the previous carbonate-buffered experiment, but still were not as consistent as the experiments that used a phosphate buffer (2nd order, k' = 3.3125, R^2 = 0.9765).

The sixth experiment, SII-O2-200-exp2, introduced one change; a better regulator. We had been constantly adjusting the regulator throughout the course of the experiments. The regulator wasn't doing its job to the precision that we required. We didn't replace the regulator, we hooked up an extra one (taken from an old gas chromatograph). The old regulator was set to a pressure of around 15 psi, and the new one (in control of the headspace pressure of the reaction vessel) was set to 0.1 kg/cm^3 (above atmospheric pressure). This change in design had a significant effect on the consistency and behavior of results (1st order, k' = 0.9948, R^2 = 0.9971). The result of a 1st order relationship is significant because that is the relationship found by Millero and Zhang in 1991. However, the results are not directly comparable to Millero and Zhang because these

experiments are at under different conditions (different reaction solution and different partial pressure of O_2).

The seventh experiment, SII-O2-200-p2deux, sought to replicate the conditions of the previous experiment, except for being run at a higher pressure (0.5 kg/cm^2). To calculate the true rate constant, experiments that differ only in their oxygen partial pressure would have to be run. It is impossible to determine a true rate constant from one experiment. The rate law for this chemical reaction, (7), because oxygen concentration is held contant, would be used to calculate the true rate constant (using experiment designs that differ ony in O_2 partial pressure).

Running repeats of the experiments at different concentrations of O_2 provides data needed to determine the true rate constant. However, SII-O2-200-p2deux gave inconsistent data and showed a 2nd order relationship with SII dropdown rather than the first order relationship seen in the previous experiment. Additionally, the reaction proceeded at a much slower rate than the previous experiment. It appeared that there were extra unknown variables that were affecting the experiment that could not be controlled for. One hypothesis is that the pressure regulators were malfunctioning, giving the reaction vessel an inconsistent headspace pressure of oxygen, reflected in increased variability of data. Another hypothesis was that the previous experiment was contaminated with an unknown trace metal that served as a catalyst for the reaction. This would explain the faster reaction rate of the previous experiment.

The experiment SII-O2-200-p2tres was run under identical conditions as the previous experiment, SII-O2-200-p2deux. The same inconsistencies were seen in these data.

Changes in the experimental setup were introduced at this time which allowed two separate experiments to take place at the same time. Two reaction vessels sit in a larger tub of water, which sits on 2 stir plates. The oxygen tank is connected to one regulator, which is set at a high pressure, and that regulator is connected to 2 different regulators, after a split. These two different regulators control the pressure in the two different reaction vessels.

The next experiment, SII-O2-200-p2arba'aah, was run under identical conditions as the previous experiments; SII-O2-200-p2deux and SII-O2-200-p2tres, except that the reaction vessel was soaked in an HCl acid bath as an additional step of the preparation in order to reduce any possible contamination by trace metals. Results from this experiment were consistent with the prior 2 experiments that did not have an acid wash step in the prep.

At the same time, experiment SII-O2-200-exp1alpha was run as a repeat of SII-O2-200-exp1 where consise 1st order behavior was seen. It was run at the same pressure (0.1 kg/cm^2), but included an acid wash step in the prep to minimize any possible trace metal contamination. It gave inconsistent results with the prior experiment it sought to replicate, showing 2nd order behavior and a much slower reaction rate.

Both experiments SII-O2-200-p2arba'ahh and SII-O2-200-exp1alpha were run at the same time. They both show the same aberration near the end of the course of experiments (a slight increase in reaction rate). This is interpreted as an effect of both reations sharing one pressure regulator, which suggests that the variability of data is a function of a poorly performing pressure regulator.

Further changes were introduced to the design at this time. A hypothesis that back end pressure on the regulators controlling the headspace pressure in the separate reaction vessels was not high enough for the regulators to function properly. A regulator capable of higher pressure was swapped into the apparatus and connected to the oxygen tank. Metal plumbing

was introduced to accommodate the resulting increase in pressure.

The next two experiments, SII-02-200-1.1bar and SII-O2-200-2bar (run by Daniel Eldridge), were run at different pressures and a test of the new apparatus. Near the beginning of the experiments, data seemed to show 1st order behavior, which switched to 2nd order later on. A hypothesis on why this behavior is happening might be that the act of sampling influences the course of the experiment. A way to test this hypothesis would be to use a peristalic pump to sample the reaction vessels which would allow for sampling without breaking the seal on the system, resulting in less impact on the experiment by the sampling.

4. Discussion

Behavior of system

Our hypothesis that the reaction vessel can fulfill its duty to the best of all reaction vessel duties is unsupported by data. In Experiments SII-O2-200-p2arba'aah and SII-O2-200-exp1alpha, which were run concurrently, in closed systems, but shared a single pressure regulator, both show the same aberration in SII dropdown. This can be easily interpreted as variation in partial pressure of oxygen, rendering moot our hypothesis that the apparatus will work properly. Suggested improvements include increasing pressure to the regulator attached to the tank and swapping out the plastic tubing for metal tubing in the high pressure zone. The pressure regulators that we used were designed to run with a high back-end pressure that was just not possible with the plastic tubing we use.

Trace metal contamination

Experiments by University of Delaware Professor Luther suggest that the oxidation of sulfur in an incredibly slow process and that the experiments by Zhang and Millero do not reveal the uncatalyzed rate constant. This is because Zhang and Millero use seawater, which includes numerous trace metals, many of which could be used in catalyzing the reaction.

In order to determine the trace-metal free kinetic rate of sulfur oxidation, the Luther group used plastic labware that was excessively sterilized in order to prevent trace metal catalysis. The found that the uncatalyzed reaction proceeds very slowly. The seawater (trace metals present) experiments by Zhang and Millero (1991) have a half-life of about 1-2 days, whereas the Luther experiments (2011) show a half-life of 55±1 days.

Error Analysis

Uncertainties present in these experiments include uncertainties of the sulfide concentrations of individual timestamps, uncertainties on the line of best fit of the sulfur concentration time series, and uncertainties arising from changes in experimental conditions. Estimates for the uncertainty of concentration measurements are obtained by analyzing samples in triplicate. The mean of the three points is taken as the value and the standard deviation is taken as the 1σ uncertainty. Uncertainty for the line of best fit is obtained by a bootstrap resampling with replacement technique and a Monte Carlo propagation of uncertainty. Our experiments performed at higher pressures systematically show greater error than the experiments performed at lower pressures.

The Monte Carlo propagation of uncertainty (Bevington and Robinson, 2003) is used to calculate the uncertainty on the slope of our functions. A randomly generated number that is within the mean and standard deviation of each point is produced for each data point. The slope of the line of best fit through these points is then calculated (k' value). This is repeated many times in order to get a good estimate of the standard deviation and mean of the slope. For this analysis, this was repeated 1,086 times (n=1,087).

The bootstrap resampling with replacement technique (Good, 2005) is slightly different. Instead of generating random numbers based on

the data, numbers are randomly selected from the data. A data set is produced with the same number of points as the original data set, but usually will contain repeats. The slope of the line of best fit will be calculated. This is repeated many times. The average of the slopes and the standard deviation is then calculated.

The bootstrap resampling with replacement technique and the Monte Carlo propagation tell us different things. The propagation will show higher variability than the resampling if there is a variable that is not controlled well during the experiments. Our data shows that.

5. Conclusions

An experimental apparatus was designed to measure SII consumption in sulfide oxidation reactions. Several modifications to the design arose during the course of the experiments. These modifications were necessary due to problems encountered that hindered the collection and quality of the data. These included modifying the initial sulfide concentration, buffers, buffer concentration, trace metal contamination, sampling affecting data, efficiency of time, and pressure regulation.

The most recent version of the apparatus addressed issues with poor pressure regulation, and efficiency of time. Issues with trace metal contamination and sampling affecting data still remain.

Future improvements to the design can be implemented. These include a refinement in cleaning procedures to fix trace metal contamination. This would entail the use of plasticware rather than borosilicate glassware (which is a possible source of trace metals) and cleaning the plasticware with nitric acid. A refinement in sampling could be implemented in the future with a peristaltic pump. The pump could be attached directly to the reaction vessel. This will allow sampling to occur without the risk of exposing the reaction vessel to sudden changes in pressure or atmospheric contamination.

Refinements in pressure control are not needed at this time due to the introduction of higher back end pressure on the regulators and the associated introduction of metal tubing to accommodate these pressures. Refinements in temperature control are not needed at this time because the reaction vessels are still submerged in the temperature controlled water bath, which is rated to ± 0.01° C precision.

With these improvements, the goal of these experiments, to accurately measure SII consumption during sulfide oxidation experiments at a constant temperature, is closer to being realized.

6. Acknowledgements

I wish to express my profound gratitude to Dr. James Farquhar and Daniel Eldridge for their seemingly infinite help, with which I have accumulated some semblance of understanding on this project. Special thanks to Alice Bowman for reviewing the manuscript from a 3rd party perspective. Additional thanks to Jonathan Lent for lending me dry socks in my time of sodden need, Kacie Baker for her hospitality, Rachel Swihart for her advice, Huan Cui for retrieving my keys from the locked lab room, Jonathan Vocke for his craftsmanship, and L. Kottke, J. Fahey, R. Eggleston, Dr. G. Liszt, and B. Molsky for general inspiration.

7. References

Bevington, P., and K. Robinson, (2003). Data Reduction and Error Analysis for the Physical Sciences. *McGraw-Hill Higher Education*, p. 190.

Canfield, D. E., J. Farquhar, et al., (2010). High isotope fractionations during sulfate reduction in a low-sulfate euxinic ocean analog. *Geology*, v. 38, p. 415-418.

Canfield, D., and A. Teske, (1996). Late Proterozoic

rise in atmospheric oxygen concentration inferred from phylogenetic and sulphur-isotope studies. *Nature*, v. 382, p. 127-132.

Chen, K. Y. and J. C. Morris, (1972). Kinetics of Oxidation of Aqueous Sulfide by O_2. *Environmental Science & Technology*, v. 6, p. 529-&.

Cline, J.D., (1969). Spectrophotometric Determination of Hydrogen Sulfide in Natural Waters. *Limnol. Oceanogr*., v. 14, p. 454-458.

Efron, B., (1979). Bootstrap Methods: Another Look at the Jacknife. *The Annals of Statistics*, v. 7, p. 1-26.

Ferdelman, T., Fossing, H., and K. Neumann, (1999). Sulfate reduction in surface sediments of the southeast Atlantic continental margin between 15°38'S and 27°57'S (Angola and Namibia). *Limnol. Oceanogr*, v. 44, p. 650-661.

Fischer, E., (1883). Bildung von Methylenblau als Reaction auf Schwefelwasswestoff. *Chem. Ber.,* v. 26, p. 2234-2236.

Good, P., (2005). Resampling Methods, 3rd edition. *Birkhäuser*, p. 8-27.

Fry, B., W. Ruf, et al., (1988). Sulfur Isotope Effects Associated with Oxidation of Sulfide by O-2 in Aqueous-Solution. *Chemical Geology,* v. 73, p. 205-210.

Jacobs, L., and S. Emerson, (1982). Trace metal solubility in an anoxic fjord. *Earth and Planetary Science Letters*, v. 60, p. 237-252.

Jørgensen, B., (1990). The sulfur cycle of freshwater sediments: Role of thiosulfate. *Limnol. Oceanogr*, v. 35, p. 1329-1342.

Jørgensen, B., and F. Bak, (1991). Pathways and Microbiology of Thiosulfate Transformations and Sulfate Reduction in a Marine Sediment (Kattegat, Denmark). *Appl. Environ. Microbiol.* v. 57, p. 847-856.

Jørgensen, B. B., H. Fossing, et al., (1991). Sulfide Oxidation in the Anoxic Black-Sea Chemocline. *Deep-Sea Research Part a-Oceanographic Research Papers*, v. 38, p. 1083-1103.

Li, X. N., W. P. Gilhooly, et al., (2010). Stable sulfur isotopes in the water column of the Cariaco Basin. *Geochimica et Cosmochimica Acta*, v. 74, p. 6764-6778.

Luther, G., Findlay, A., MacDonald, D., Owings, S., Hanson, T., Beinart, R., and Girguis, P., (2011). Thermodynamics and kinetics of sulfide oxidation by oxygen: a look at inorganically controlled reactions and biologically mediated processes in the environment. *Frontiers in Microbiology*, v. 2, no. 62.

Morse, J., and J. Cornwell, (1987). Analysis and distribution of iron sulfide minerals in recent anoxic marine sediments. *Marine Chemistry*, v. 22, p. 55-69.

Morse, J., Millero, F., Cornwell, J., and Rickard, D., (1987). The chemistry of the hydrogen sulfide and iron sulfide systems in natural waters. *Earth-Science Reviews*, v. 24, p. 1-42.

O'Brien, D. J. and F. B. Birkner, (1977). Kinetics of Oxygenation of Reduced Sulfur Species in Aqueous-Solution. *Environmental Science & Technology*, v. 11, p. 1114-1120.

Sakai, H., (1957). Fractionation of sulphur isotopes in nature. *Geochemica et Cosmochimica Acta*, v. 12, p. 150-169.

Schoen, R., and R. Rye, (1970). Sulfur Isotope Distribution in Solfataras, Yellowstone National Park. *Science*, New Series, v. 170, p. 1082-1084.

Steudel, R., Holdt, G., and Nagorka, R., (1986). Sulfur Compounds .104 On the Autoxidation of Aqueous Sodium Polysulfide. *Zeitschrift fur Naturforschung Section B-A Journal of Chemical Sciences,* v. 41, p. 1519-1522.

Steudel, R., (1996). Mechanism for the Formation of Elemental Sulfur from Aqueous Sulfide in Chemical -and Microbiological Desulfurization Processes. *Ind. Eng. Chem. Res*, v. 35, p. 1417-1423.

Strickland, J., and T. Parsons, (1968). A manual of seawater analysis. *Bull Fisheries Res. Board Can.* 167. 311 p.

Xu, Y. and M. A. A. Schoonen, (1995). The Stability of Thiosulfate in the Presence of Pyrite in Low-Temperature Aqueous-Solutions. *Geochimica et Cosmochimica Acta,* v. 59, p. 4605-4622.

Zeebe, R., (2011). Marine Carbonate Chemistry. *The Encyclopedia of Earth*, retrieved from http://www.eoearth.org/view/article/154468

Zerkle, A. L., A. Kamyshny, et al., (2010). Sulfur cycling in a stratified euxinic lake with moderately high sulfate: Constraints from quadruple S isotopes. *Geochimica et Cosmochimica Acta*, v. 74, p. 4953-4970.

Zhang, J. Z. and F. J. Millero, (1991). The Rate of Sulfite Oxidation in Seawater. *Geochimica et Cosmochimica Acta*, v. 55, p. 677-685.

Zhang, J. Z. and F. J. Millero, (1993). The Products from the Oxidation of H_2S in Seawater. *Geochimica et Cosmochimica Acta*, v. 57, p. 1705-1718.

Zopfi, J., (2004). Distribution and fate of sulfur intermediates – sulfite, tetrathionate, thiosulfate, and elemental sulfur – in marine sediments. *Geological Society of America Special Papers*, v. 379, p. 97-116.

8. Appendix

Timeline/Summary

Experiment Name	Dates	Changes introduced
SII-O2-exp1	7/25 – 7/28/2013	Initial experiment, phosphate buffer, 0.1M, 5 psi
SII-O2-exp2	8/9 – 8/12/2013	Doubled Buffer Concentration
SII-O2-exp2α	8/13 – 8/16/2013	Repeat
SII-O2-Carb-exp1	8/28 - 8/30/2013	Switch to carbonate buffer, 0.1M
SII-O2-200-exp1	9/11 – 9/14/2013	Reduce sulfide - 200 mM, buffer - 5mM, 1.5 psi
SII-O2-200-exp2	9/18 – 9/21/2013	Better Regulator, 0.1 kg/cm^2
SII-O2-200-p2deux	10/15 – 10/17/2013	Repeat at 0.5 kg/cm^2
SII-O2-200-p2tres	10/18 – 10/21/2013	Repeat
SII-O2-200-p2arba'aah	10/22 – 10/25/2013	Repeat
SII-O2-200-exp1alpha	10/22 – 10/25/2013	Repeat at 0.1 kg/cm^2
SII-O2-200-1.1bar	11/5 – 11/8/2013	Improved pressure regulation, 0.1 kg/cm^2
SII-O2-200-2bar	11/5 – 11/8/2013	Repeat at 1 kg/cm^2

Graphs

Results from the experiments is provided below in graph form. Trendlines going through the data points are calculated by plotting the inverse concentration vs. time (for 2nd order behavior) and the natural log of concentration vs. time (for 1st order behavior). The Nth order behavior that has the higher R^2 value is shown next to the graph and used to calculate the trendline within the data points. When the Nth order behavior is ambiguous, both trendlines are shown. Some sets of data are better explained with two separate trendlines (SII-O2-200-1.1bar and SII-O2-200-2bar).

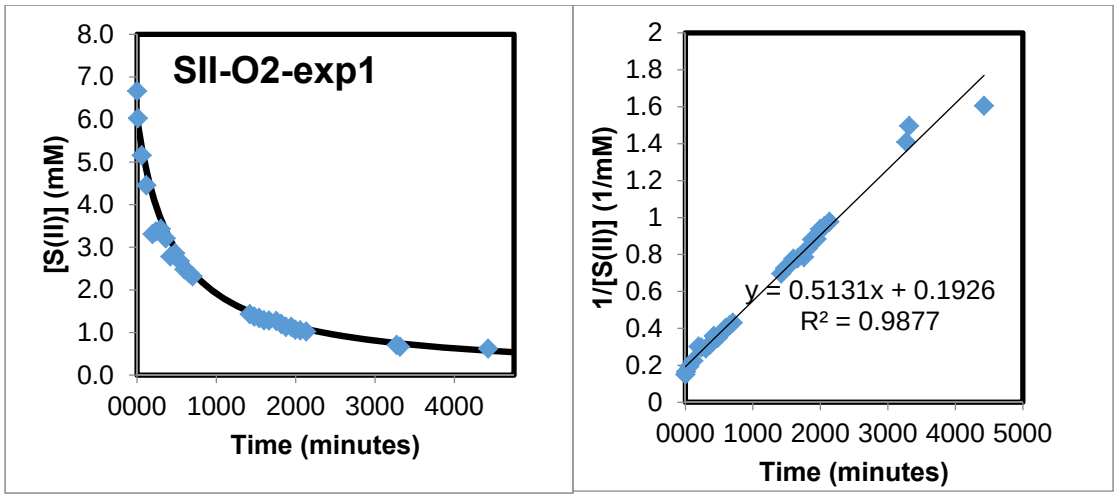

Figure 2: General Results from SII-O2-exp1

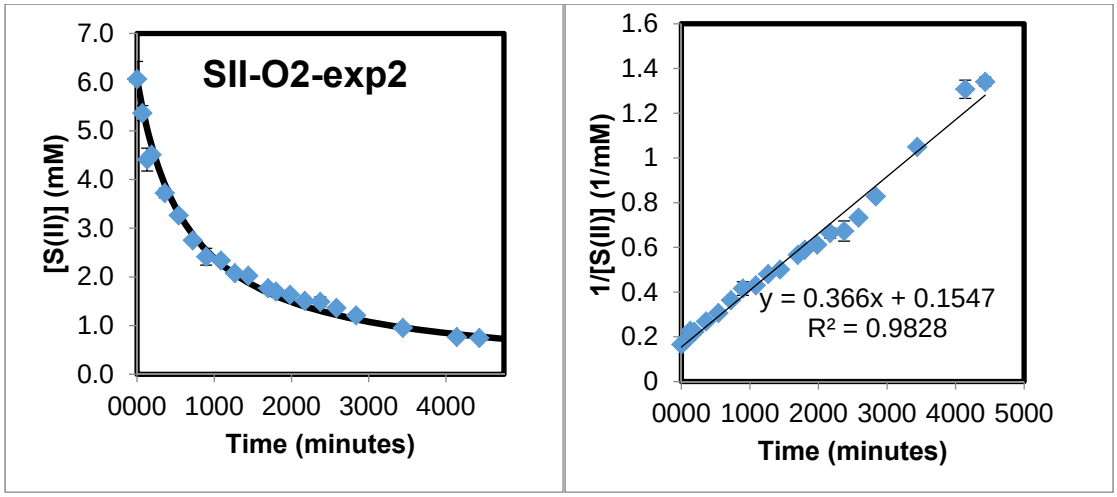

Figure 3: General Results from SII-O2-exp2

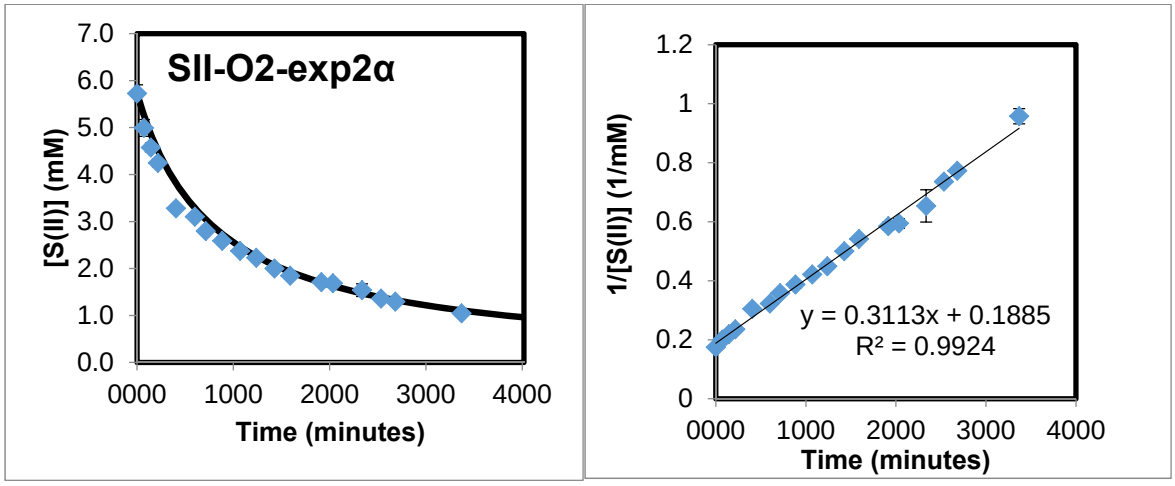

Figure 4: General Results from SII-O2-exp2α

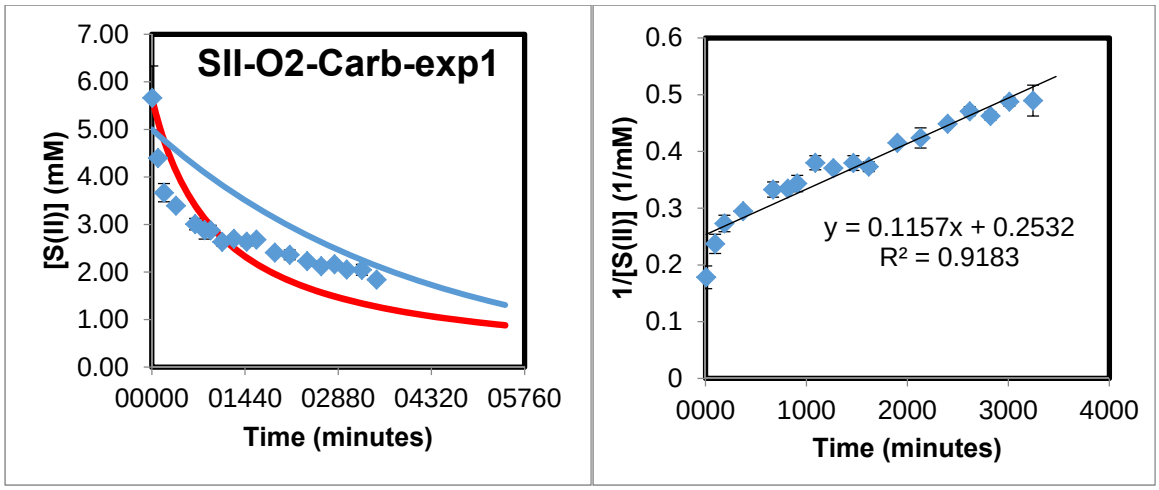

Figure 5: General Results from SII-O2-Carb-exp1. Red trendline: 2nd order fit, blue trendline: 1st order fit.

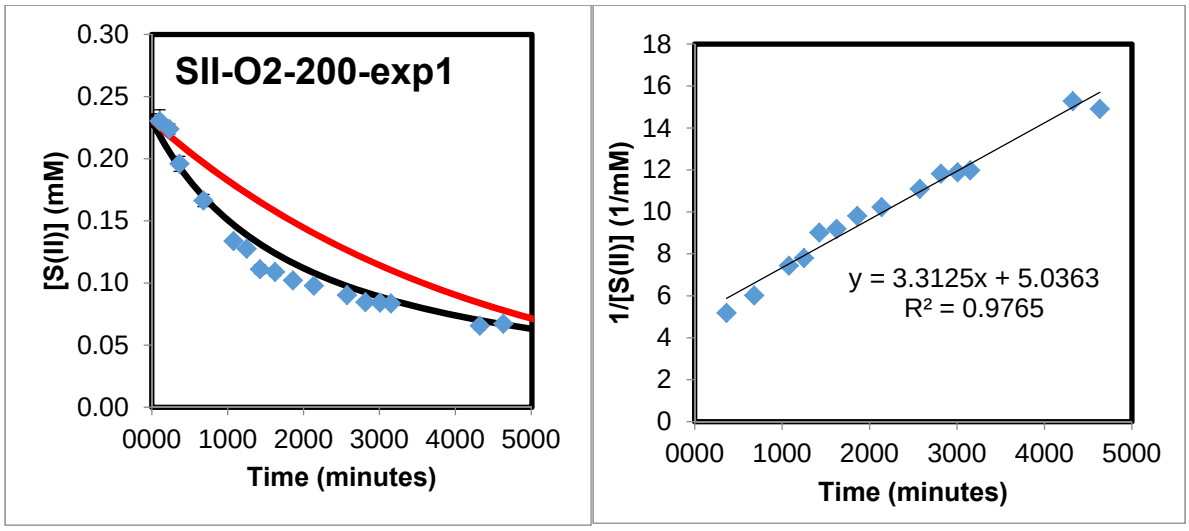

Figure 6: Generalized results from SII-O2-200-exp1. Red trendline: 2nd order fit, blue trendline: 1st order fit.

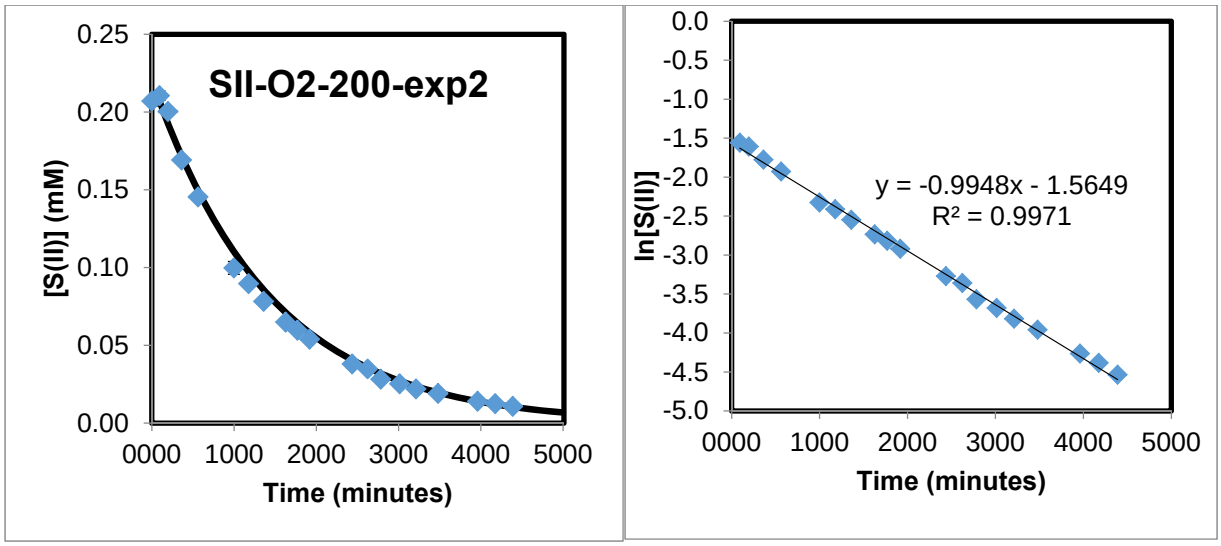

Figure 7: Generalized results from SII-O2-200-exp2. These data are unusual in that they show 1st order behavior, and are quite compelling. It is thought that this experiment was contaminated with trace metals that catalyzed the experiment.

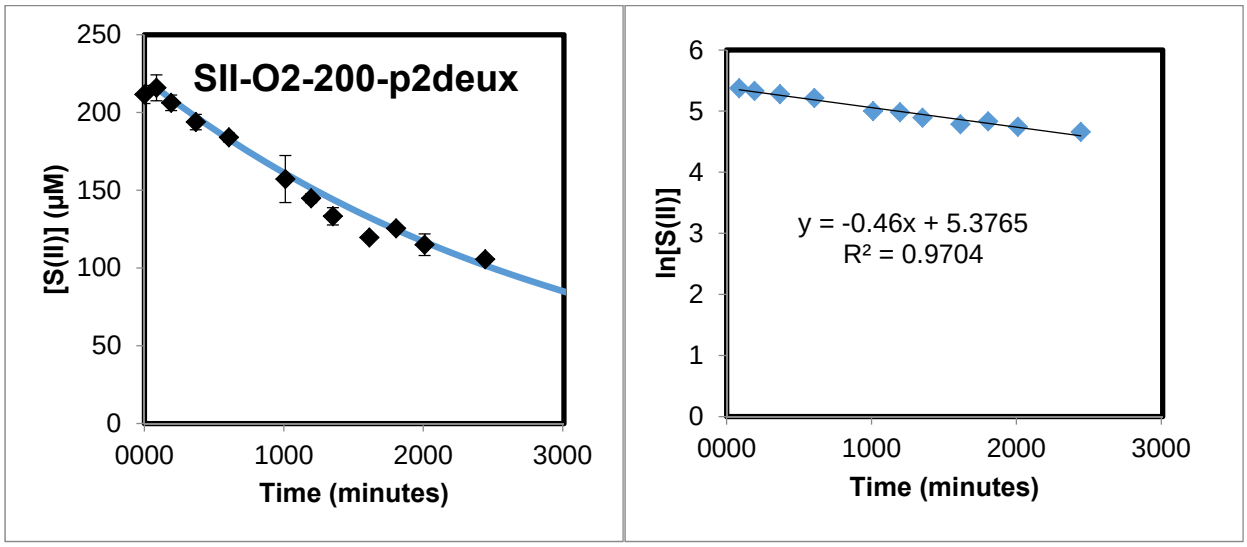

Figure 8: Generalized results from SII-O2-200-p2deux

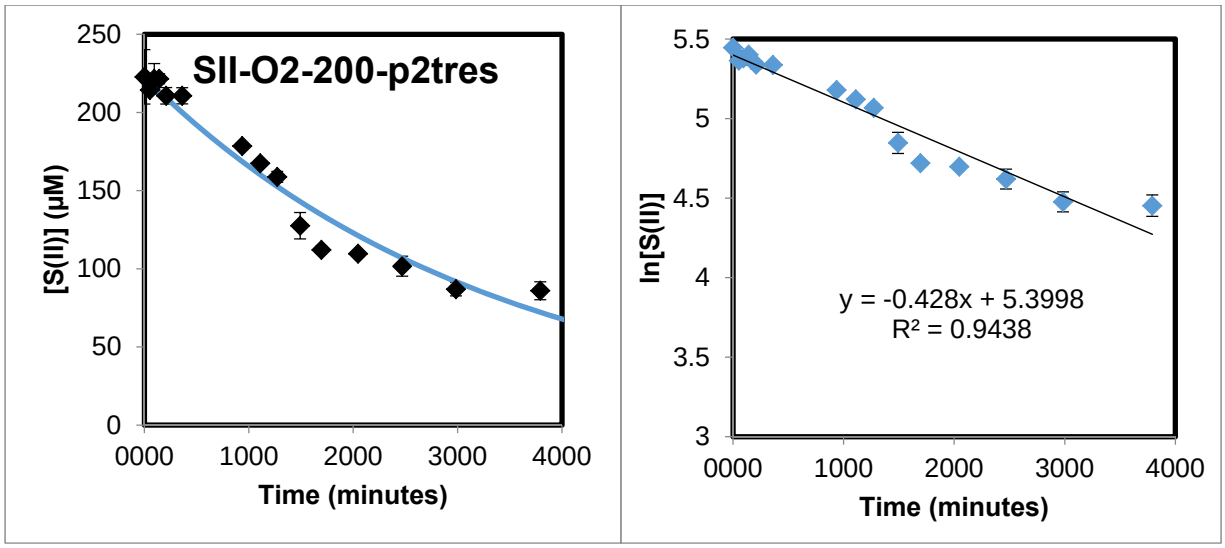

Figure 9: Generalized results from SII-O2-200-p2tres

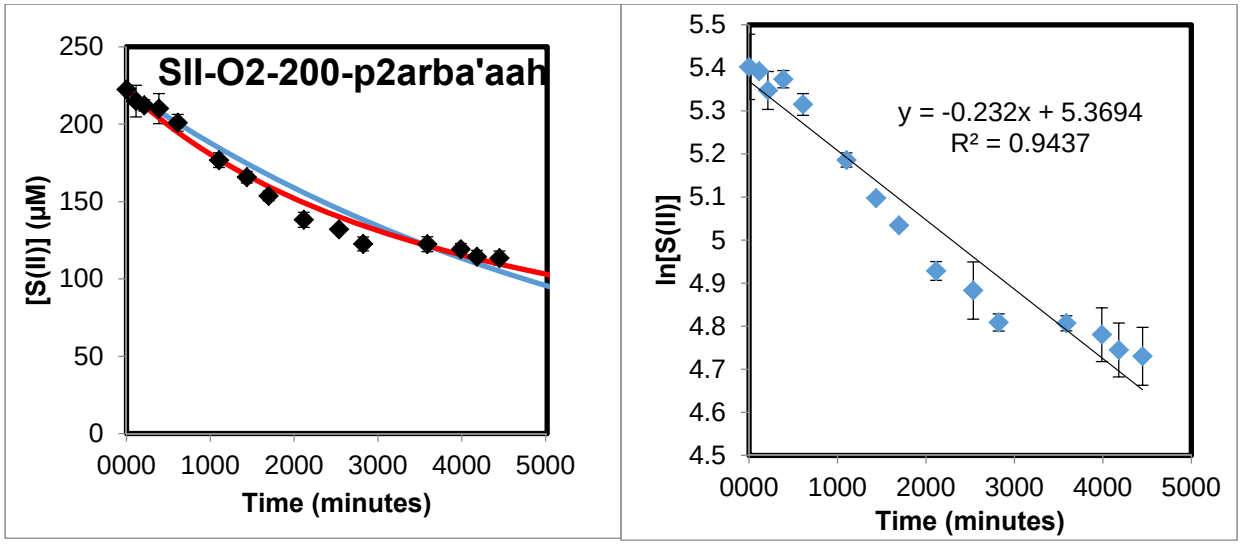

Figure 10: Generalized Results from SII-O2-200-p2arba'aah. Arba'aah is the Arabic word for four. Red trendline: 2nd order fit, blue trendline: 1st order fit.

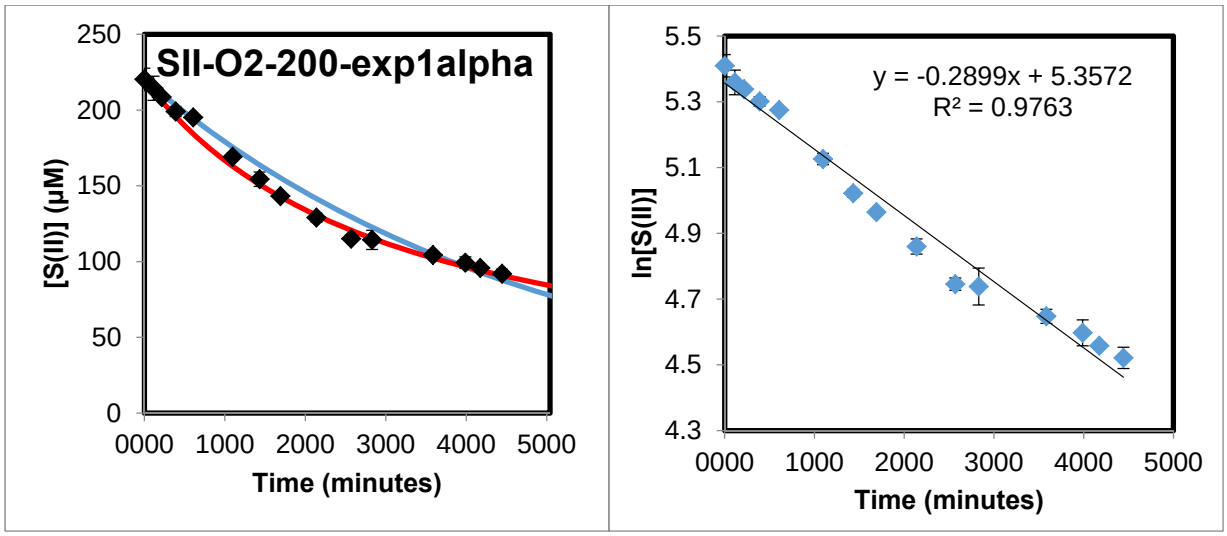

Figure 11: Generalized Results from SII-O2-200-exp1alpha. Red trendline: 2nd order fit, blue trendline: 1st order fit.

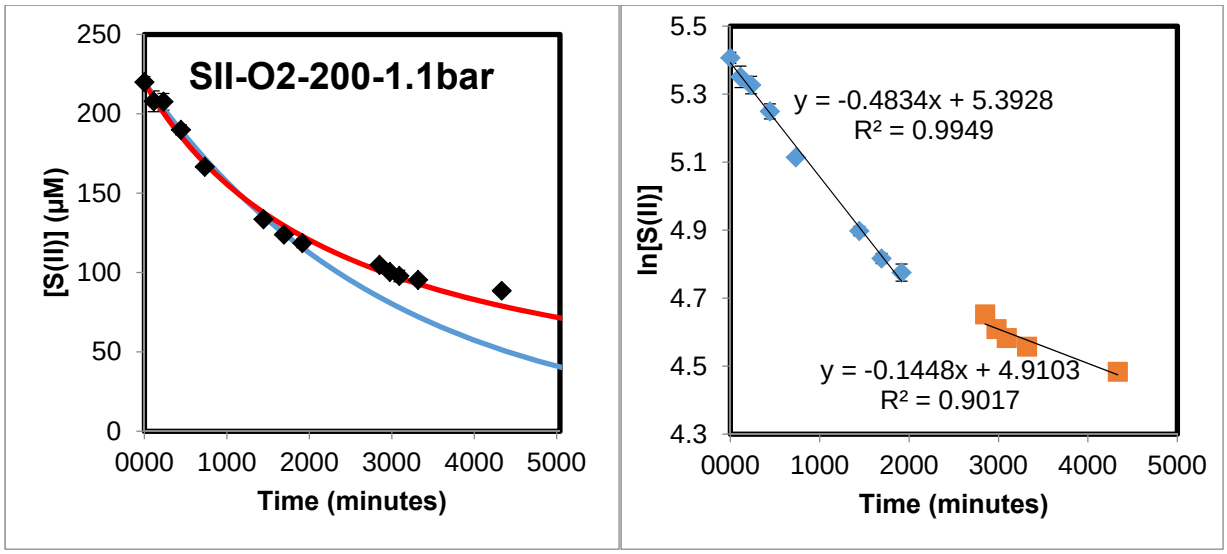

Figure 12: Generalized Results from SII-O2-200-1.1bar. Red trendline: y = -0.1448x + 4.9103, blue trendline: y = -0.4834x + 5.3928.

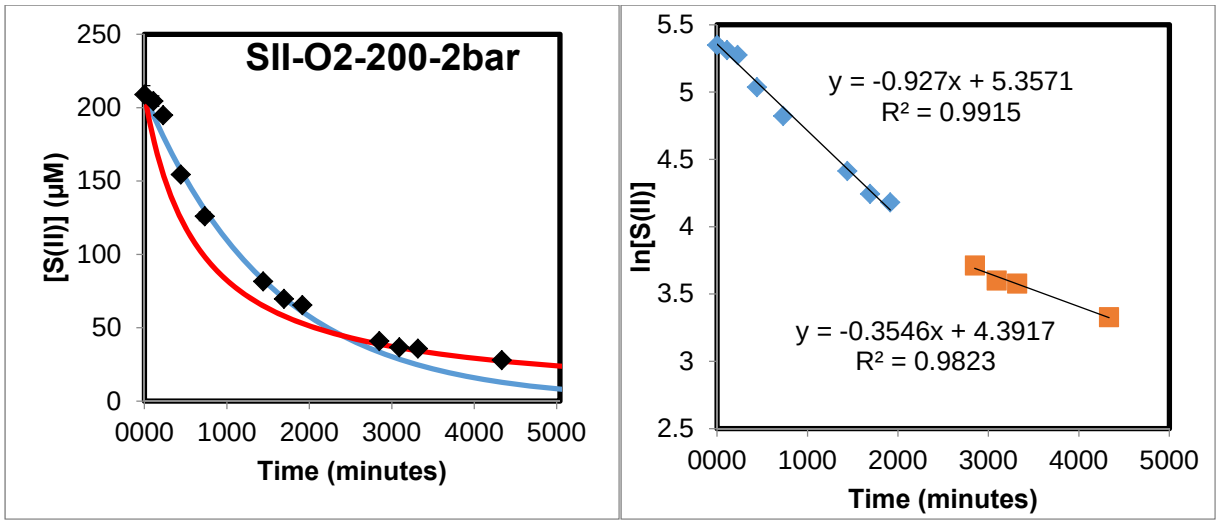

Figure 13: Generalized Results from SII-O2-200-2bar. Red trendline: y = -0.3546x + 4.3917. Blue trendline: y = -0.927x + 5.3571.

Statistics

Experiment	Slope (rate constant) 1/days	Uncertainty (propagated from measurement uncertainty) (2 sigma)	Uncertainty (estimated from Monte Carlo Resampling) (2 sigma)
SII-O2-exp2	-0.64	0.01	0.10
SII-O2-exp2alpha	-0.69	0.02	0.11
SII-O2-Carb-exp1	-0.33	0.03	0.09
SII-O2-200-exp1	-0.41	0.01	0.10
SII-O2-200-exp2	-0.99	0.01	0.03
SII-O2-200-p2deux	-0.46	0.03	0.05
SII-O2-200-p2tres	-0.43	0.04	0.09
SII-O2-200-p2arbaaah	-0.23	0.02	0.03
SII-O2-200-exp1alpha	-0.29	0.01	0.03
SII-O2-200-1.1bar	-0.33	0.01	0.06
SII-O2-200-2bar	-0.73	0.02	0.12

Control 1	
Experimental Time (min)	**Actual Concentration (micromolar)**
00000	**9693**
00061	**6139**
00120	**6013**
00179	**5097**
00284	**6076**
00336	**5939**
00408	**6024**
00458	**6045**
01529	**5823**
01597	**5897**
01718	**5971**
01875	**5834**
02935	**5539**
07464	**5697**
07477	**5855**
07500	**6076**
07512	**5823**
08721	**5560**
08753	**5708**
08780	**5571**

SII-O2-exp1		
Experimental Time (min)	**Actual Concentration (micromolar)**	**ln[conc]**
00000	**6669**	8.81
00010	**6032**	8.70
00059	**5158**	8.55
00118	**4457**	8.40
00195	**3313**	8.11
00237	**3372**	8.12
00300	**3432**	8.14
00362	**3210**	8.07
00420	**2784**	7.93
00480	**2860**	7.96
00539	**2676**	7.89
00597	**2482**	7.82
00659	**2390**	7.78
00701	**2320**	7.75
01421	**1435**	7.27
01480	**1375**	7.23
01540	**1343**	7.20
01600	**1286**	7.16
01663	**1283**	7.16
03103	**839**	6.73
01756	**1272**	7.15
01817	**1199**	7.09
01877	**1134**	7.03
01944	**1131**	7.03
01996	**1066**	6.97
02057	**1050**	6.96
02133	**1023**	6.93
03272	**710**	6.56
03315	**668**	6.50
04425	**623**	6.43

		Slope	-0.64	
	Uncertainty (propagated from measurement uncertainty) (2 sigma		0.01	
SII-O2-exp2	Uncertainty (estimated from Monte Carlo Resampling) (2 sigma)		0.10	
Average Exp Time (min)	**Average Actual Conc. (millimolar)**	**Standard dev. (2 sigma)**	**Avg. ln[conc]**	**Uncert. Ln[conc]**
Plotted	*Plotted*	*Plotted*	*Plotted*	
00000	**6.1**	**0.7**	8.71	**0.12**
00069	**5.4**	**0.3**	8.59	**0.06**
00131	**4.4**	**0.5**	8.39	**0.11**
00188	**4.5**	**0.2**	8.41	**0.03**
00359	**3.7**	**0.2**	8.22	**0.05**
00540	**3.3**	**0.1**	8.09	**0.03**
00722	**2.75**	**0.03**	7.92	**0.01**
00896	**2.4**	**0.3**	7.79	**0.14**
01086	**2.34**	**0.02**	7.76	**0.02**
01266	**2.08**	**0.02**	7.64	**0.01**
01440	**2.02**	**0.02**	7.61	**0.05**
01697	**1.77**	**0.03**	7.48	**0.02**
01800	**1.70**	**0.03**	7.44	**0.02**
01981	**1.63**	**0.03**	7.40	**0.02**
02171	**1.5**	**0.1**	7.32	**0.07**
02373	**1.5**	**0.2**	7.31	**0.13**
02583	**1.4**		7.22	
02836	**1.2**		7.10	
03441	**0.95**	**0.02**	6.86	**0.02**
04140	**0.77**	**0.05**	6.64	**0.06**
04431	**0.75**	**0.02**	6.61	**0.03**

		Slope	-0.69	
	Uncertainty (propagated from measurement uncertainty) (2 sigma		0.02	
SII-O2-exp2alpha	Uncertainty (estimated from Monte Carlo Resampling) (2 sigma)		0.11	
Average Exp Time (min)	**Average Actual Conc. (millimolar)**	**Standard dev. (1 sigma)**	**Avg. ln[conc]**	**Uncert. Ln[conc]**
Plotted	*Plotted*	*Plotted*	*Plotted*	
00000	**5.7**	**0.4**	8.65	**0.06**
00071	**5.0**	**0.4**	8.52	**0.07**
00143	**4.6**	**0.2**	8.43	**0.04**
00217	**4.2**	**0.2**	8.35	**0.04**
00404	**3.3**	**0.1**	8.10	**0.02**
00601	**3.1**	**0.1**	8.04	**0.03**
00714	**2.8**	**0.1**	7.94	**0.03**
00884	**2.6**	**0.2**	7.86	**0.06**
01070	**2.4**	**0.1**	7.77	**0.05**
01237	**2.2**	**0.1**	7.71	**0.02**
01426	**2.0**	**0.1**	7.60	**0.04**
01590	**1.8**	**0.0**	7.52	**0.01**
01914	**1.7**	**0.1**	7.44	**0.04**
02034	**1.7**	**0.1**	7.43	**0.05**
02336	**1.5**	**0.3**	7.34	**0.17**
02534	**1.36**	**0.01**	7.21	**0.01**
02681	**1.3**	**0.0**	7.17	**0.02**
03368	**1.0**	**0.1**	6.95	**0.05**

		Slope	-0.33	
	Uncertainty (propagated from measurement uncertainty) (2 sigma		0.03	
SII-O2-Carb-exp1	Uncertainty (estimated from Monte Carlo Resampling) (2 sigma)		0.09	
Average Exp Time (min)	**Average Actual Conc. (millimolar)**	**Standard dev. (1 sigma)**	**Avg. ln[conc]**	**Uncert. Ln[conc]**
Plotted	*Plotted*	*Plotted*	*Plotted*	
00006	**5.7**	**1.3**	8.64	**0.23**
00095	**4.40**	**0.05**	8.39	**0.01**
00187	**3.7**	**0.4**	8.21	**0.11**
00373	**3.4**	**0.1**	8.13	**0.02**
00669	**3.0**	**0.2**	8.01	**0.08**
00815	**2.9**	**0.4**	7.97	**0.03**
00908	**2.9**	**0.2**	7.96	**0.08**
01088	**2.6**	**0.2**	7.88	**0.06**
01267	**2.7**	**0.1**	7.90	**0.03**
01464	**2.6**	**0.2**	7.88	**0.07**
01617	**2.7**	**0.1**	7.89	**0.05**
01901	**2.4**	**0.1**	7.79	**0.02**
02131	**2.4**	**0.2**	7.77	**0.09**
02399	**2.23**	**0.02**	7.71	**0.01**
02617	**2.1**	**0.1**	7.66	**0.03**
02824	**2.2**	**0.1**	7.68	**0.03**
03010	**2.1**	**0.1**	7.63	**0.03**
03244	**2.0**	**0.2**	7.62	**0.11**
03472	**1.8**	**0.1**	7.52	**0.08**

		Slope	-0.41	
	Uncertainty (propagated from measurement uncertainty) (2 sigma		0.01	
SII-O2-200-exp1	Uncertainty (estimated from Monte Carlo Resampling) (2 sigma)		0.10	
Average Exp Time (min)	**Average Actual Conc. (micromolar)**	**Standard dev. (1 sigma)**	**Avg. ln[conc]**	**Uncert. Ln[conc]**
Plotted	*Plotted*	*Plotted*	*Plotted*	
-00001	**231**	**11**	5.44	**0.05**
00102	**235**		5.46	**0.06**
00230	**224**	**8**	5.41	**0.04**
00364	**196**	**12**	5.28	**0.05**
00681	**166**	**10**	5.11	**0.06**
01077	**134**	**4**	4.90	**0.03**
01249	**128**	**3**	4.85	**0.02**
01425	**111**	**7**	4.71	**0.06**
01622	**109**	**6**	4.69	**0.06**
01859	**102**	**3**	4.63	**0.03**
02136	**98**	**5**	4.58	**0.05**
02573	**90**	**2**	4.50	**0.02**
02815	**85**	**1**	4.44	**0.01**
03006	**84**	**2**	4.43	**0.02**
03151	**83**	**3**	4.42	**0.03**
04323	**66**	**6**	4.18	**0.10**
04633	**67.2**	**0.4**	4.21	**0.01**

		Slope	-0.99	
	Uncertainty (propagated from measurement uncertainty) (2 sigma		0.01	
SII-O2-200-exp2	Uncertainty (estimated from Monte Carlo Resampling) (2 sigma)		0.03	
Average Exp Time (min)	**Average Actual Conc. (micromolar)**	**Standard dev. (1 sigma)**	**Avg. ln[conc]**	**Uncert. Ln[conc]**
Plotted	*Plotted*	*Plotted*	*Plotted*	
00000	**207**	**7**	**5.33**	**0.03**
00093	**211**	**6**	**5.35**	**0.03**
00195	**200**	**4**	**5.30**	**0.02**
00361	**169**	**2**	**5.13**	**0.01**
00561	**145**	**3**	**4.98**	**0.02**
00998	**100**	**8**	**4.60**	**0.08**
01176	**90**	**4**	**4.50**	**0.04**
01360	**78**	**1**	**4.36**	**0.01**
01626	**65.0**	**0.4**	**4.17**	**0.01**
01769	**60**	**2**	**4.09**	**0.04**
01917	**54**	**2**	**3.99**	**0.03**
02435	**38**	**6**	**3.64**	**0.15**
02624	**35**	**1**	**3.55**	**0.02**
02783	**28**	**1**	**3.34**	**0.02**
03012	**25**	**1**	**3.23**	**0.05**
03210	**22**	**1**	**3.09**	**0.03**
03479	**19.1**	**0.2**	**2.95**	**0.01**
03961	**14.1**	**0.2**	**2.64**	**0.02**
04174	**13**	**1**	**2.53**	**0.05**
04389	**11**	**1**	**2.37**	**0.09**

		Slope	-0.46	
	Uncertainty (propagated from measurement uncertainty) (2 sigma		0.03	
SII-O2-200-p2deux	Uncertainty (estimated from Monte Carlo Resampling) (2 sigma)		0.05	
Average Exp Time (min)	**Average Actual Conc. (micromolar)**	**Standard dev. (1 sigma)**	**Avg. ln[conc]**	**Uncert. Ln[conc]**
Plotted	*Plotted*	*Plotted*	*Plotted*	
0000	**212**	**12**	**5.35**	**0.06**
0086	**216**	**17**	**5.37**	**0.08**
0192	**206**	**10**	**5.33**	**0.05**
0368	**194**	**10**	**5.28**	**0.05**
0605	**184**	**6**	**5.21**	**0.03**
1011	**157**	**30**	**5.00**	**0.04**
1196	**145**	**6**	**4.98**	**0.05**
1352	**133**	**11**	**4.89**	**0.08**
1614	**120**	**2**	**4.78**	**0.02**
1805	**125**	**4**	**4.83**	**0.03**
2009	**115**	**14**	**4.74**	**0.12**
2444	**106**	**3**	**4.66**	**0.02**

		Slope	-0.43	
	Uncertainty (propagated from measurement uncertainty) (2 sigma		0.04	
SII-O2-200-p2tres	Uncertainty (estimated from Monte Carlo Resampling) (2 sigma)		0.09	
Average Exp Time (min)	**Average Actual Conc. (micromolar)**	**Standard dev. (1 sigma)**	**Avg. ln[conc]**	**Uncert. Ln[conc]**
Plotted	*Plotted*	*Plotted*	*Plotted*	
-0000	**223**	**35**	**5.45**	**0.15**
0052	**214**	**3**	**5.36**	**0.01**
0094	**222**	**19**	**5.38**	**0.09**
0141	**222**	**6**	**5.40**	**0.04**
0208	**211**	**11**	**5.34**	**0.05**
0361	**211**	**10**	**5.34**	**0.03**
0937	**179**	**3**	**5.18**	**0.01**
1110	**167**	**3**	**5.12**	**0.02**
1272	**159**	**7**	**5.07**	**0.04**
1492	**128**	**17**	**4.85**	**0.13**
1695	**112**	**4**	**4.72**	**0.04**
2047	**110**	**4**	**4.70**	**0.03**
2469	**102**	**13**	**4.62**	**0.12**
2985	**87**	**9**	**4.48**	**0.13**
3792	**86**	**11**	**4.45**	**0.13**

		Slope	-0.23	
	Uncertainty (propagated from measurement uncertainty) (2 sigma		0.02	
SII-O2-200-p2arbaaah	Uncertainty (estimated from Monte Carlo Resampling) (2 sigma)		0.03	
Average Exp Time (min)	**Average Actual Conc. (micromolar)**	**Standard dev. (1 sigma)**	**Avg. ln[conc]**	**Uncert. Ln[conc]**
Plotted	*Plotted*	*Plotted*	*Plotted*	
0000	**222**	**6**	**5.40**	**0.03**
0114	**215**	**20**	**5.39**	**0.09**
0213	**212**	**7**	**5.35**	**0.03**
0388	**210**	**19**	**5.37**	**0.02**
0611	**201**	**11**	**5.32**	**0.05**
1103	**177**	**9**	**5.19**	**0.05**
1436	**166**	**8**	**5.10**	**0.01**
1696	**154**	**6**	**5.03**	**0.04**
2114	**138**	**10**	**4.93**	**0.07**
2535	**132**	**4**	**4.88**	**0.03**
2823	**123**	**9**	**4.81**	**0.07**
3588	**122**	**10**	**4.81**	**0.08**
3988	**119**	**7**	**4.78**	**0.06**
4180	**114**	**8**	**4.74**	**0.10**
4449	**113**	**9**	**4.73**	**0.08**

		Slope	-0.29	
	Uncertainty (propagated from measurement uncertainty) (2 sigma		0.01	
SII-O2-200-exp1alpha	Uncertainty (estimated from Monte Carlo Resampling) (2 sigma)		0.03	
Average Exp Time (min)	**Average Actual Conc. (micromolar)**	**Standard dev. (1 sigma)**	**Avg. ln[conc]**	**Uncert. Ln[conc]**
Plotted	*Plotted*	*Plotted*	*Plotted*	
-0000	**220**	**15**	**5.41**	**0.07**
0112	**214**	**16**	**5.36**	**0.08**
0215	**209**	**4**	**5.34**	**0.02**
0388	**199**	**7**	**5.30**	**0.03**
0607	**195**	**3**	**5.28**	**0.01**
1095	**169**	**5**	**5.13**	**0.03**
1432	**154**	**10**	**5.02**	**0.02**
1689	**143**	**3**	**4.96**	**0.02**
2137	**129**	**6**	**4.86**	**0.05**
2569	**115**	**4**	**4.75**	**0.04**
2829	**114**	**13**	**4.74**	**0.11**
3584	**104**	**4**	**4.65**	**0.04**
3988	**99**	**8**	**4.60**	**0.08**
4174	**96**	**2**	**4.56**	**0.02**
4443	**92**	**6**	**4.52**	**0.06**

		Slope	-0.33	
	Uncertainty (propagated from measurement uncertainty) (2 sigma		0.01	
SII-O2-200-1.1bar	Uncertainty (estimated from Monte Carlo Resampling) (2 sigma)		0.06	
Average Exp Time (min)	**Average Actual Conc. (micromolar)**	**Standard dev. (2 sigma)**	**Avg. ln[conc]**	**Uncert. Ln[conc]**
Plotted	*Plotted*	*Plotted*	*Plotted*	*2 sigma*
-0000	**220**	**7**	**5.41**	**0.03**
0113	**208**	**13**	**5.35**	**0.06**
0232	**208**	**11**	**5.33**	**0.05**
0442	**190**	**6**	**5.25**	**0.04**
0731	**167**	**2**	**5.11**	**0.01**
1443	**134**	**3**	**4.90**	**0.03**
1692	**124**	**3**	**4.82**	**0.03**
1916	**119**	**6**	**4.78**	**0.05**
2850	**105**	**2**	**4.65**	**0.02**
2977	**100**	**2**	**4.61**	**0.02**
3092	**98**	**7**	**4.58**	**0.07**
3318	**95**	**1**	**4.56**	**0.01**
4333	**89**	**2**	**4.48**	**0.02**

		Slope	-0.73	
	Uncertainty (propagated from measurement uncertainty) (2 sigma		0.02	
SII-O2-200-2bar	Uncertainty (estimated from Monte Carlo Resampling) (2 sigma)		0.12	
Average Exp Time (min)	**Average Actual Conc. (micromolar)**	**Standard dev. (1 sigma)**	**Avg. ln[conc]**	**Uncert. Ln[conc]**
Plotted	*Plotted*	*Plotted*	*Plotted*	
-0000	**209**	**12**	**5.35**	**0.06**
0109	**205**	**7**	**5.31**	**0.03**
0227	**195**	**5**	**5.28**	**0.02**
0441	**154**	**3**	**5.04**	**0.02**
0731	**126**	**6**	**4.82**	**0.05**
1440	**82**	**4**	**4.41**	**0.03**
1692	**70**	**2**	**4.24**	**0.05**
1914	**65**	**3**	**4.18**	**0.05**
2849	**41**	**1**	**3.71**	**0.02**
3091	**37**	**1**	**3.60**	**0.01**
3316	**36**	**1**	**3.58**	**0.02**
4333	**28**	**3**	**3.33**	**0.09**

Misc.

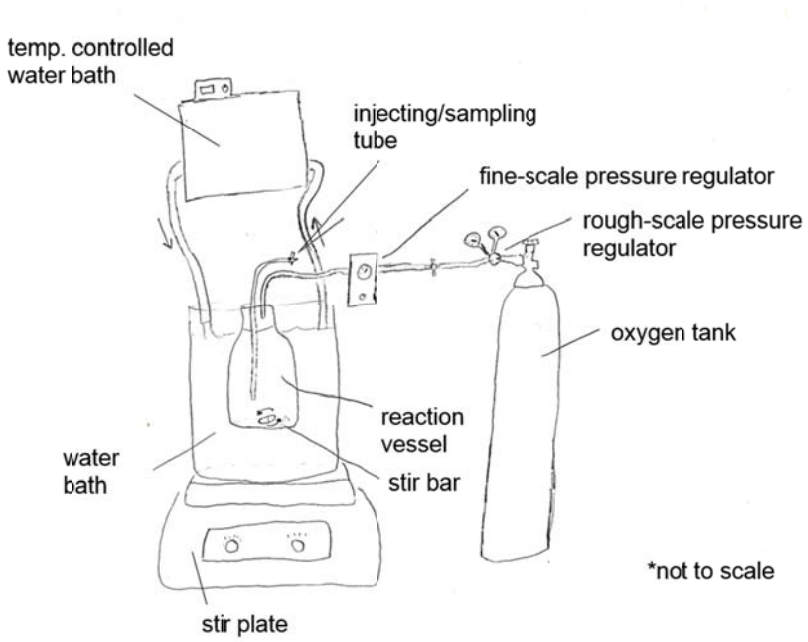

Figure 14: Generalized Illustration of Experimental apparatus

Honor Code

I pledge on my honor that I have not given or received any unauthorized help on this assignment.

Noah C. Bowman 11-27-2013